Alternative Reassortment Events Leading to Transmissible H9N1 Influenza Viruses in the Ferret Model

J. Brian Kimble, Matthew Angel, Hongquan Wan,* Troy C. Sutton, Courtney Finch, Daniel R. Perez

Department of Veterinary Medicine, University of Maryland College Park and Virginia-Maryland Regional College of Veterinary Medicine, College Park, Maryland, USA

Influenza A H9N2 viruses are common poultry pathogens that occasionally infect swine and humans. It has been shown previously with H9N2 viruses that reassortment can generate novel viruses with increased transmissibility. Here, we demonstrate the modeling power of a novel transfection-based inoculation system to select reassortant viruses under *in vivo* selective pressure. Plasmids containing the genes from an H9N2 virus and a pandemic H1N1 (pH1N1) virus were transfected into HEK 293T cells to potentially generate the full panel of possible H9 reassortants. These cells were then used to inoculate ferrets, and the population dynamics were studied. Two respiratory-droplet-transmissible H9N1 viruses were selected by this method, indicating a selective pressure in ferrets for the novel combination of surface genes. These results show that a transfection-based inoculation system is a fast and efficient method to model reassortment and highlight the risk of reassortment between H9N2 and pH1N1 viruses.

Influenza A H9N2 virus began appearing in domestic poultry in the late 1980s. Throughout most of the 1990s, these viruses remained in domestic and wild bird populations and displayed typical avian receptor and species specificity (1–4). However, in the later part of the decade, the virus began showing more human-like receptor specificity, and in 1998, the first swine H9N2 virus was isolated (5). A year later, the first human H9N2 virus was isolated in Hong Kong (6). Since then there have been several more isolations of H9N2 virus from humans. However, the minimal clinical symptoms associated with the subtype combined with seroprevalence surveys suggest the possibility of a higher incidence in humans (7, 8).

The segmentation of the influenza virus genome allows the exchange of genetic material upon coinfection of the same cell in a process called reassortment. Natural reassortment of H9N2 viruses can have significant impacts on human health (9). Phylogenetic analyses showed that the highly pathogenic H5N1 virus from 1997 and the G1-like H9N2 virus have common internal genes, indicating a past reassortment event (10). This suggests a contribution from an H9N2 virus to the internal genes of the HPAI H5N1 virus that infected humans (10). Genetic drift has caused distinct lineages of H9N2 virus to emerge in Eurasia, and between three and five Eurasian H9N2 lineages have been proposed (11–13). Recent data have shown that H9N2 reassortment, together with adaptive mutations, can generate novel reassortant viruses that are more transmissible and more pathogenic in mammalian models than the parental viruses (14, 15). The emergence of the 2009 pandemic H1N1 (pH1N1) virus further heightened concern, as H9N2 viruses have been shown to be compatible for reassortment with the newly emerged pandemic virus (16, 17). The recent H7N9 virus outbreak in China further highlights the importance of H9N2 viruses in reassortment, as the outbreak virus is itself a reassortant with an H9N2 virus (18). This virus, containing internal genes from an avian H9N2 virus, infected more than 130 people and was associated with more than 40 fatalities (19, 20).

With eight segments in each virus, studying reassortment represents a large combinatorial problem, with 256 distinct genome constellations existing between any virus pairs. Previous studies investigating reassortment have used several methods: blunt force, arbitrary genome selection, or coinfections. The first two methods use directed reassortment to create all or a select few of the total possible combinations, respectively (16, 17). The first of the two methods is time intensive, and although it may yield detailed information on genomic compatibility, it reveals little about competition or population dynamics. The second method generates a minimal set of constellations through directed reassortment. This may answer a number of other biologically important questions but poorly mimics the complexity of natural reassortment. Finally, some studies have selected for viruses by coinfecting either cell culture or an appropriate animal model (21, 22). While this may better simulate a natural coinfection, replication of the inoculated viruses may outcompete less abundant, but potentially more fit, reassortant constellations. In this study, we developed a 15-plasmid transfection-based inoculation (TBI) system to quickly and efficiently mimic a reassortment event between an H9N2 virus and pH1N1 virus in ferrets. This system potentially generates all possible reassortant viruses in a biologically relevant animal model under *in vivo* selective pressure and without competition from high-titer wild-type inoculated viruses.

MATERIALS AND METHODS

Fifteen-plasmid TBI. HEK 293T cells were transfected with 1 μg each of 15 plasmids containing the surface gene segments from A/ferret/Maryland/P10-UMD/2008 (H9N2) virus (15), the internal genes from A/guinea fowl/HK/WF10 (H9N2) virus, and 7 gene segments from A/NL/602/2009 (H1N1) virus (23) excluding segment 4 (hemagglutinin [HA]) to ensure the resultant virus was an H9. Transfections were done using TransIt LT-1 (Mirus, Madison, WI) in 6-well cell culture plates. The transfected cells were lifted 24 h posttransfection (p.t.) and collected in the transfection supernatant. Seronegative ferrets were inoculated with 1 ml
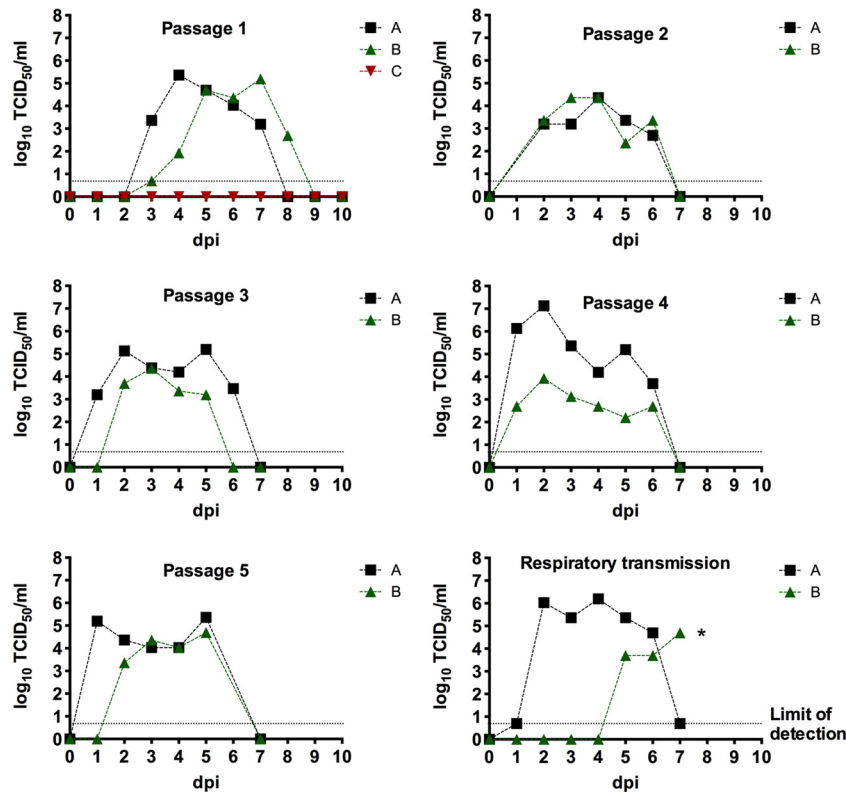
FIG 1 Transfection-based inoculation and subsequent serial passage of viral lineages show consistent infectivity. Three ferrets were inoculated with transfected cells in P1. Daily nasal wash samples were titrated by $TCID_{50}$ in MDCK cells, and the nasal wash sample with the highest titer was used to inoculate the next passage through P5. Respiratory-contact ferrets were added at 1 day p.i. of P5. Lineage A grew to higher titers and faster than lineage B. Lineage C failed to infect the initial ferret. *, study terminated prior to complete virus clearance by the RC ferret infected with lineage B virus. dpi, days p.i.

of transfected cells/supernatant, which corresponded to one well of cells. The ferrets were monitored for signs of disease and sampled daily by nasal washes with 1 ml of PBS. The nasal wash fluids were tested for viral antigen with FluDetect (Synbiotics Corp. San Diego, CA), aliquoted, and stored at −80°C.

Virus selection. Selection of the fittest virus was determined by serial passage of the viral population in ferrets in the following manner. The transfected cells were used to inoculate passage 1 (P1) ferrets. The day of peak shedding was determined by 50% tissue culture infective dose ($TCID_{50}$) titration, and 700 μl of the nasal wash sample was used to directly inoculate P2 ferrets. Based on the shedding curve of P2 ferrets, samples from 4 days postinoculation (p.i.) were used to inoculate the next passage of ferrets out to P5. Ferrets for RCP5 were added to the cages of P5 ferrets in a manner to allow only respiratory contact (RC) at 1 day p.i.

Animal studies. All studies were approved by the Animal Care and Use Committee of the University of Maryland (protocol R-09-93). Three- to 7-month-old female ferrets were purchased from Triple F farms (Sayer, PA). The ferrets were quarantined for 7 days in an animal biosafety level 2 (ABSL2) facility. All animals were implanted with temperature transponders (Bio Medics, Seaford, DE) to identify individual ferrets and record body temperature. Sera were used to determine the naivety of each ferret prior to experimentation. The ferrets were lightly anesthetized with ketamine (20 mg/kg of body weight) and xylazine (1 mg/kg) via an intramuscular injection prior to all manipulations.

Limiting dilutions. Transfection supernatant was passed in MDCK cells once for 48 h. The cell culture supernatant was diluted 10-fold from 10^{-1} to 10^{-8} across a 96-well plate containing MDCK cells. After 72 h, an HA assay was performed, and the well that was inoculated with the most diluted sample that still resulted in infection was selected and assumed to have the most homogeneous virus population. The process was repeated

12 times down the 96-well plate, thus selecting 12 different virus populations. The supernatants from the 12 selected wells were then partially sequenced to identify the eight gene segments present.

Deep sequencing. The nasal wash sample from the day of highest shedding for P1 and RCP5 for each lineage was selected for sequencing. Specifically, lineage A P1 at 4 days p.i., lineage A RCP5 at 4 days p.i., lineage B P1 at 7 days p.i., and lineage B RCP5 at 7 days p.i. were chosen. Viral sequencing was performed on ferret nasal wash fluids passaged once in MDCK cells at a multiplicity of infection (MOI) of 0.1 to enrich for viral RNA and eliminate interfering host RNA. RNA extraction and barcoded sequence-independent, single-primer amplification (SISPA) libraries were constructed essentially as previously described with minor modifications (24, 25). Briefly, supernatants were clarified by centrifugation at 3,000 × *g* for 15 min at 4°C and incubated in a DNase I (10-U)-RNase A (50-U) mixture at 37°C for 30 min. TRIzol-LS (Invitrogen, Grand Island, NY) was used to inactivate the nuclease mixture and lyse the virus. Samples were processed following the manufacturer's recommendations until the phase separation, at which point 100% ethanol was added to the aqueous phase at a final concentration of ≥40% and purified through an RNeasy Mini spin column (Qiagen, Gaithersburg, MD). First and second strands were transcribed with barcoded random hexamers and amplified with barcoded primers. The amplified libraries were size selected with 0.7 volumes of Ampure XP beads (Beckman Coulter, Inc., Brea, CA) and sequenced on the GS Junior 454 sequencer following the manufacturer's recommendations and omitting the nebulization step. Newbler software was used to perform assembly, and the average read depth was greater than 300 reads per base for each sample. A second set of samples representing nasal washes from the second-highest day of shedding for each passage and lineage were sequenced in a manner similar to that described
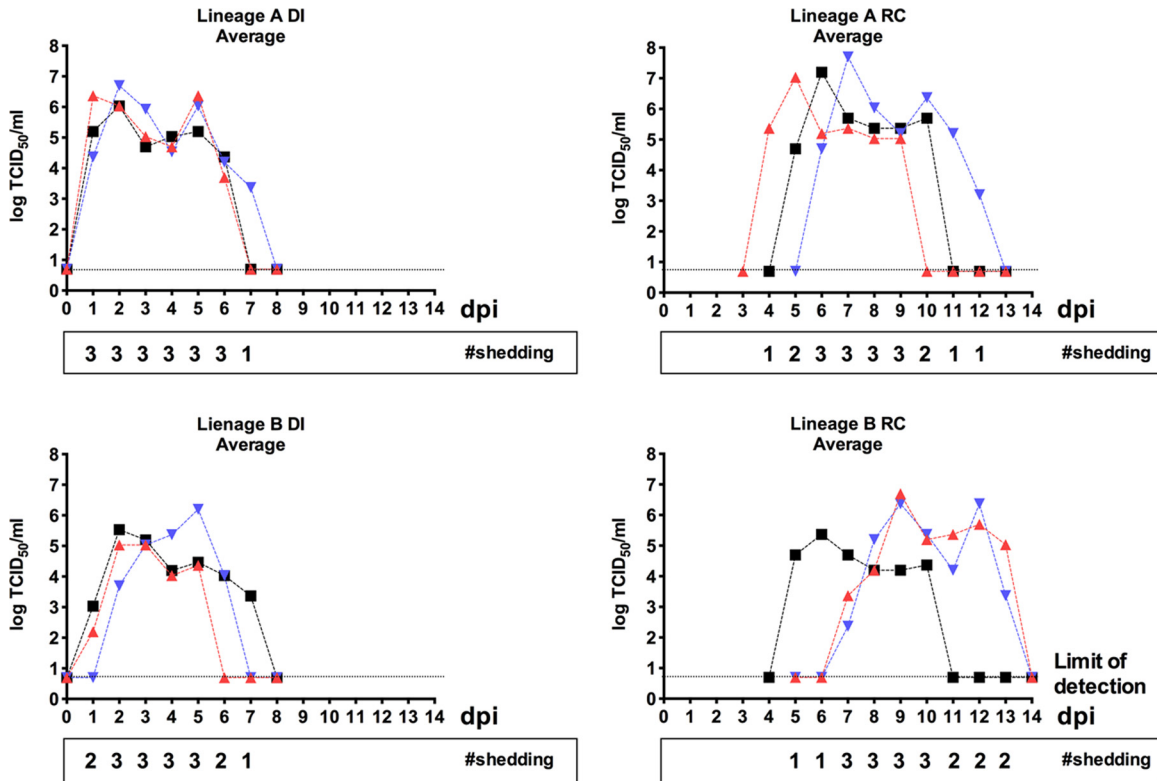
FIG 2 Lineage A and B viruses are transmitted by respiratory droplets in ferrets. Three directly inoculated (DI) ferrets per lineage were inoculated with 10^5 TCID$_{50}$ of P4 virus from nasal wash. At 1 day p.i., a single RC ferret was added to each DI ferret (total, three per lineage). All ferrets were subjected to daily nasal washes, and the samples were titrated by TCID$_{50}$ in MDCK cells. The colors, symbols, and numbers indicate matched pairs (e.g., the black square DI1 was housed with the black square AC1).

above. The genetic constellations and mutations matched what was reported for the first set of samples.

RESULTS AND DISCUSSION

Three ferrets were inoculated intranasally with cells transfected with 15 plasmids and monitored by nasal washes. Two of the three ferrets became infected and began shedding virus at 3 days p.i. (Fig. 1). Based on the potential viral diversity, we assumed the ferrets were shedding a mixed population of viruses. To select for a single or more homogeneous virus population, serial passages were performed via direct inoculation of nasal washes from 5 days p.i. into a naive ferret. This process was repeated until the nasal washes had been serially passaged 5 times to create two distinct lineages (A and B) originating from the initially inoculated animals. These ferrets displayed typical shedding profiles, with peak titers between 10^4 and 10^6 TCID$_{50}$/ml nasal wash and viral clearance after 6 or 7 days (Fig. 1). To assess transmissibility, one RC ferret was added to the isolator of each P5 ferret at 1 day p.i. in such a way that physical contact was eliminated but the airspace was shared. Both lineage A and B RC ferrets became infected; however, due to time constraints, the experiment was terminated prior to clearance of the infection by the RC ferret in the lineage B group. To fully evaluate transmission, 3 ferrets were inoculated with either lineage A or B P4 nasal wash fluid, recapitulating the fifth passage. At 1 day p.i., a respiratory-contact (RCP5) ferret was added to the isolator of each directly inoculated animal as described above. The two lineages were transmitted efficiently, as all three RCP5 ferrets in each group became infected, although the

lineage A virus was transmitted slightly faster and grew to slightly higher titers than the lineage B virus (Fig. 2).

Next, 454 pyrosequencing was performed on the samples with the highest titers from P1 and RCP5 from both lineages to identify the genetic constellation of viruses in selected samples. Sequencing was then performed on a second set of samples with the second-highest level of shedding. All genetic constellations and mutations seen in the highest-titer sample were confirmed in the samples with the second-highest titers. Sequence analysis revealed that both lineages resulted in an H9N1 virus with internal genes from both H9N2 and pH1N1 viruses (Table 1). Both lineages contained pH1N1 origin PB2, NP, and NA gene segments and H9N2 origin PA, HA, and NS gene segments. The two lineages differed in the PB1 and M segments. These two segments were of pH1N1 origin in lineage A and of H9N2 origin in lineage B. The selection of an H9N1 virus is consistent with previous studies (16, 26).

Sequencing revealed a number of mutations throughout the genomes of both lineages. Lineage A accrued four mutations during the six ferret passages: one each in PB2 (D253N), PA (K26E), HA (HA1 domain, S254N; 263 in H3 numbering), and NS (D2N) (Table 2). The PB2 D253N substitution is in the NP binding and cap binding domain (27). This mutation has been described in an H9N2 backbone to increase replication and pathogenicity in mice (28). The PB2 D253N substitution was not identified in the P1 sample but was seen in 100% of reads in the RCP5 sample. We also identified the D2N mutation in NS1 and NEP. This mutation has been identified with increased virus titers, beta interferon (IFN-β)

TABLE 1 Sequencing indicates that TBI results in the selection of H9N1 variants from a mixed population[a]

Deep sequencing	PB2	PB1	PA	HA	NP	NA	M	NS
Lineage A P1	■	■	□	□	■	■	■	□
Lineage A RCP5	■	■	□	□	■	■	■	□
Lineage B P1	■	□	□	□	■	□	□	□
Lineage B RCP5	■	□	□	□	■	□	□	□
Tissue culture selection	77	97	65	100	7	13	77	81

Limiting dilution	PB2	PB1	PA	HA	NP	NA	M	NS
1	□	■	□	□	■	■	□	□
2	□	□	□	□	■	■	□	□
3	□	□	■	□	■	□	■	□
4	■	□	■	■	■	■	■	■
5	□	■	■	■	■	■	■	■
6	□	□	□	■	□	□	□	□
7	□	■	□	□	■	■	□	□
8	□	□	□	□	■	■	□	□
9	■	■	□	■	■	□	□	■
10	□	□	□	□	■	■	□	□
11	■	□	□	□	■	■	□	□
12	▨	□	■	□	■	■	▨	▨
% w/ H9 var.	69.3	100	30.7	100	7.7	7.7	76.9	69.3

[a] The numbers indicate the percentages of sequencing reads that map to the H9 variant of each gene segment. Black shading indicates pH1N1 origin, while white indicates an H9 origin. Gray shading indicates a mixed population.

induction, weight loss, pathology, and mortality in mice in an H3N2 background (29, 30). We found D2N in 60% of sequencing reads in RCP5 and in 0% of reads in P1. The other three mutations have not been associated with any phenotypic changes (27, 31).

Lineage B accumulated six mutations during ferret passage. One mutation arose in PB2 (A707T), PA (silent), HA (HA1, S319C; 328 in H3 numbering), and M (E95K in M2), and two mutations arose in PB1 (D120N and D439E) (Table 2). None of these mutations has been associated with any specific phenotypic changes. However, the PB2 A707T mutation lies in the PB1 binding domain and may modulate binding of a PB1 and a PB2 with different origins (31). We did not identify the mutation in P1, but it was found at 100% in RCP5. The PB1 D120N mutation lies in a region of PB1 with no described function, but the base pair substitution (G382A) does result in a 3-amino-acid (aa) truncation of PB1-F2 (90 aa to 87 aa) (27, 32). The 87-aa PB1-F2 variant is often found in nature. No functional difference between the 90-aa and 87-aa PB1-F2 variants has been described (32). This mutation was found in 30% of P1 reads and 100% of RCP5 reads. Finally, the HA S319C mutation lies in the p2 position of the HA cleavage site. The RSSR/G motif is fairly conserved in Eurasian avian H9 isolates, but the p2 and p3 sites are far more flexible in swine isolates (33–35). We detected this mutation in only 20% of reads from the RCP5 sample. However, the S319C mutation is inconsistent with currently available H9 HA sequences deposited in GenBank. In fact, a cysteine in such a position is likely detrimental to virus fitness and might in part explain the low virus titers and slow transmission kinetics of the lineage B strain in ferrets. It is also tempting to speculate that, just as with the presence of defective interfering particles, some influenza virus strains may contain subpopulation variants encoding defective protein products that ultimately modulate virulence and/or transmission.

Pathologically, these viruses are similar to seasonal influenza virus (36). Alveolitis and interstitial pneumonia, characterized by evident inflammatory infiltration of neutrophils, lymphocytes, and macrophages, were observed in the lungs from both groups at 3 days p.i. and 5 days p.i. (Fig. 3). Congestion was more evident in the lungs at 3 days p.i. than at 5 days p.i. in both groups, while infiltration in the lung from the lineage B group (Fig. 3E) was more severe than in the lung from the lineage A group (Fig. 3A) at 3 days p.i. No evident lesion appeared in the tracheas. Additionally, the ferrets showed mild signs of disease. Typical signs were mild fever, moderate body weight loss, and mild lethargy.

Lineage A virus consistently grew faster and to higher titers and transmitted more efficiently than lineage B virus (Fig. 1 and 2).

TABLE 2 Multiple mutations induced by serial passages in lineage A and B viruses

Gene origin_gene segment	Nucleotide change	% of reads[a]		Amino acid change	H3 no.	Location	Effect
		P1	RCP5				
Lineage A							
pH1N1_PB2	G784A	5	100	D253N		NP binding domain; cap binding domain	Increases titer and pathogenicity in H9N2
WF10_PA	A100G	0	92	K26E		Endonuclease	Unknown
P10_HA|	G847A	0	100	S254N	263	HA1 stalk	Unknown
WF10_NS	G30A	0	60	D2N			Increased titers, IFN-β induction, pathology and mortality in mice
Lineage B							
pH1N1_PB2	G2146A	0	100	A707T		PB1 binding domain; Impα5-interacting domain	Unknown
WF10_PB1	G382A	30	100	D120N		PB1-F2 early termination; truncated by 3 aa	Unknown
WF10_PB1	T1341A	0	97	D439E		No known functional domain	Unknown
WF10_PA	C909A	0	98	Silent			
P10_HA|	A1041T	0	20	S319C	328	HA1 cleavage site	Unknown
WF10_M|	G996A	0	100	E95K		Cytoplasmic domain M2	Unknown

[a] Percentages of reads that contain each mutation by 454 sequencing.

species (21, 37, 38). Indeed, lineage A contains the pH1N1 M segment and showed more efficient infectivity and transmission.

Transfection with 15 plasmids is theoretically capable of producing 128 genetically distinct viruses. To ensure our transfection produced a mixed population, we used deep sequencing of MDCK cell-passed transfection supernatant to confirm the presence of all 15 gene segments (Table 1). While no segment was completely selectively lost, partial selection was observed for each segment after 48 h in MDCK cells. In general, the tissue culture pressure partially selected the pH1N1 PB2, PB1, HA, M, and NS and H9N2 PA, NP, and NA gene segments (Table 1). Additionally, transfection supernatants were passaged by limiting dilutions in tissue culture to produce 11 individual viruses and one mixed population as determined by Sanger sequencing. The results indicated that both H9N2 origin and pH1N1 origin segments were found in at least one of the dilutions, with the exceptions of the pH1N1 HA (not included in the original transfection) and the pH1N1 PB1. However, we identified the pH1N1 PB1 in a virus from the ferrets (Table 1), confirming the viability of all included plasmids. These results indicate that all constellations were theoretically possible and that the end-result viruses were selected from the most fit segments derived from the initial 15-plasmid-transfected inoculum.

The deep sequencing and limiting dilutions of the tissue culture population showed selective pressure on the virus after only one passage. Lineages A and B differed from the tissue culture lineages in three and one segment, respectively (Table 1). This highlights the potential issue with tissue culture-based methods or selection, as the selective pressure from tissue culture skews the results compared to *in vivo* selective pressure. The results also highlight two other ways in which TBI outperforms previous methods of selection. The genetic constellation of P1 samples is identical to that of RCP5 samples (Table 1). This indicates that the selection process was completed in a single passage by 4 days p.i. Coinfection studies typically take multiple passages and require weeks of work and a large number of animals. Similarly, creating and testing each possible reassortant is a time-consuming prospect that requires large numbers of animals. TBI may rapidly select a single reassortant virus *in vivo* from a mixed population in as little as 4 days from a single animal. A similar approach can be implemented to ascertain the gene constellation that would most likely lead to more efficient respiratory-droplet transmission of other avian influenza viruses in mammals.

FIG 3 Both H9N1 reassortants exhibit pathogenicity similar to that of seasonal influenza virus. Ferrets were inoculated with 10^6 TCID$_{50}$ of MDCK cell-passed RCP5 lineage A or B virus. Tissues were collected at 3 or 5 days p.i. in formalin, cut into 5-μm sections, and stained with hematoxylin and eosin (H&E). (A and C) Lung and trachea collected from a lineage A ferret at 3 days p.i. (B and D) Lung and trachea collected from a lineage A ferret at 5 days p.i. (E and G) Lung and trachea collected from a lineage B ferret at 3 days p.i. (F and H) Lung and trachea collected from a lineage B ferret at 5 days p.i. (I and J) Lung (I) and trachea (J) from naive ferrets served as controls.

Mutational analysis revealed two mutations in lineage A (PB2 D253N and NS1/NEP D2N) that are known to increase infectivity and pathogenicity in other viral backgrounds (28, 29). While these changes could affect the phenotype, there is evidence that the differing M segments have a large effect, as well. Previous studies have found that the pH1N1 M segment allows higher infectivity and increased transmissibility in multiple backbones and multiple model

REFERENCES

1. **Alexander DJ.** 2000. A review of avian influenza in different bird species. Vet. Microbiol. **74:**3–13. http://dx.doi.org/10.1016/S0378-1135(00)00160-7.
2. **Lee CW, Song CS, Lee YJ, Mo IP, Garcia M, Suarez DL, Kim SJ.** 2000. Sequence analysis of the hemagglutinin gene of H9N2 Korean avian influenza viruses and assessment of the pathogenic potential of isolate MS96. Avian Dis. **44:**527–535. http://dx.doi.org/10.2307/1593091.
3. **Naeem K, Ullah A, Manvell RJ, Alexander DJ.** 1999. Avian influenza A subtype H9N2 in poultry in Pakistan. Vet. Rec. **145:**560. http://dx.doi.org/10.1136/vr.145.19.560.
4. **Perk S, Panshin A, Shihmanter E, Gissin I, Pokamunski S, Pirak M, Lipkind M.** 2006. Ecology and molecular epidemiology of H9N2 avian influenza viruses isolated in Israel during 2000-2004 epizootic. Dev. Biol. 201–209.

5. **Peiris JS, Guan Y, Markwell D, Ghose P, Webster RG, Shortridge KF.** 2001. Cocirculation of avian H9N2 and contemporary "human" H3N2 influenza A viruses in pigs in southeastern China: potential for genetic reassortment? J. Virol. **75:**9679–9686. http://dx.doi.org/10.1128/JVI.75.20.9679-9686.2001.

6. **Peiris M, Yuen KY, Leung CW, Chan KH, Ip PL, Lai RW, Orr WK, Shortridge KF.** 1999. Human infection with influenza H9N2. Lancet **354:** 916–917. http://dx.doi.org/10.1016/S0140-6736(99)03311-5.

7. **Pawar SD, Tandale BV, Raut CG, Parkhi SS, Barde TD, Gurav YK, Kode SS, Mishra AC.** 2012. Avian influenza H9N2 seroprevalence among poultry workers in Pune, India, 2010. PLoS One **7:**e36374. http://dx.doi.org/10.1371/journal.pone.0036374.

8. **Wang M, Fu C-X, Zheng B-J.** 2009. Antibodies against H5 and H9 avian influenza among poultry workers in China. N. Engl. J. Med. **360:**2583–2584. http://dx.doi.org/10.1056/NEJMc0900358.

9. **Xie Q, Yan Z, Ji J, Zhang H, Liu J, Sun Y, Li G, Chen F, Xue C, Ma J, Bee Y.** 2012. Complete genome sequence of a novel H9N2 subtype influenza virus FJG9 strain in China reveals a natural reassortant event. J. Virol. **86:**10240–10241. http://dx.doi.org/10.1128/JVI.01623-12.

10. **Guan Y, Shortridge KF, Krauss S, Webster RG.** 1999. Molecular characterization of H9N2 influenza viruses: were they the donors of the "internal" genes of H5N1 viruses in Hong Kong? Proc. Natl. Acad. Sci. U. S. A. **96:**9363–9367. http://dx.doi.org/10.1073/pnas.96.16.9363.

11. **Dong G, Luo J, Zhang H, Wang C, Duan M, Deliberto TJ, Nolte DL, Ji G, He H.** 2011. Phylogenetic diversity and genotypical complexity of H9N2 influenza A viruses revealed by genomic sequence analysis. PLoS One **6:**e17212. http://dx.doi.org/10.1371/journal.pone.0017212.

12. **Fusaro A, Monne I, Salviato A, Valastro V, Schivo A, Amarin NM, Gonzalez C, Ismail MM, Al-Ankari AR, Al-Blowi MH, Khan OA, Maken Ali AS, Hedayati A, Garcia Garcia J, Ziay GM, Shoushtari A, Al Qahtani KN, Capua I, Holmes EC, Cattoli G.** 2011. Phylogeography and evolutionary history of reassortant H9N2 viruses with potential human health implications. J. Virol. **85:**8413–8421. http://dx.doi.org/10.1128/JVI.00219-11.

13. **Guo YJ, Krauss S, Senne DA, Mo IP, Lo KS, Xiong XP, Norwood M, Shortridge KF, Webster RG, Guan Y.** 2000. Characterization of the pathogenicity of members of the newly established H9N2 influenza virus lineages in Asia. Virology **267:**10. http://dx.doi.org/10.1006/viro.1999.0115.

14. **Sorrell EM, Wan H, Araya Y, Song H, Perez DR.** 2009. Minimal molecular constraints for respiratory droplet transmission of an avian-human H9N2 influenza A virus. Proc. Natl. Acad. Sci. U. S. A. **106:**7565–7570. http://dx.doi.org/10.1073/pnas.0900877106.

15. **Wan H, Sorrell EM, Song H, Hossain MJ, Ramirez-Nieto G, Monne I, Stevens J, Cattoli G, Capua I, Chen LM, Donis RO, Busch J, Paulson JC, Brockwell C, Webby R, Blanco J, Al-Natour MQ, Perez DR.** 2008. Replication and transmission of H9N2 influenza viruses in ferrets: evaluation of pandemic potential. PLoS One **3:**e2923. http://dx.doi.org/10.1371/journal.pone.0002923.

16. **Kimble JB, Sorrell E, Shao H, Martin PL, Perez DR.** 2011. Compatibility of H9N2 avian influenza surface genes and 2009 pandemic H1N1 internal genes for transmission in the ferret model. Proc. Natl. Acad. Sci. U. S. A. **108:**12084–12088. http://dx.doi.org/10.1073/pnas.1108058108.

17. **Sun Y, Qin K, Wang J, Pu J, Tang Q, Hu Y, Bi Y, Zhao X, Yang H, Shu Y, Liu J.** 2011. High genetic compatibility and increased pathogenicity of reassortants derived from avian H9N2 and pandemic H1N1/2009 influenza viruses. Proc. Natl. Acad. Sci. U. S. A. **108:**4164–4169. http://dx.doi.org/10.1073/pnas.1019109108.

18. **Parry J.** 2013. H7N9 avian flu infects humans for the first time. BMJ **346:**f2151. http://dx.doi.org/10.1136/bmj.f2151.

19. **Gao R, Cao B, Hu Y, Feng Z, Wang D, Hu W, Chen J, Jie Z, Qiu H, Xu K, Xu X, Lu H, Zhu W, Gao Z, Xiang N, Shen Y, He Z, Gu Y, Zhang Z, Yang Y, Zhao X, Zhou L, Li X, Zou S, Zhang Y, Yang L, Guo J, Dong J, Li Q, Dong L, Zhu Y, Bai T, Wang S, Hao P, Yang W, Han J, Yu H, Li D, Gao GF, Wu G, Wang Y, Yuan Z, Shu Y.** 2013. Human infection with a novel avian-origin influenza A (H7N9) virus. N. Engl. J. Med. **368:**1888–1897. http://dx.doi.org/10.1056/NEJMoa1304459.

20. **Kageyama T, Fujisaki S, Takashita E, Xu H, Yamada S, Uchida Y, Neumann G, Saito T, Kawaoka Y, Tashiro M.** 2013. Genetic analysis of novel avian A(H7N9) influenza viruses isolated from patients in China, February to April 2013. Euro Surveill. **18:**20453. http://www.eurosurveillance.org/ViewArticle.aspx?ArticleId=20453.

21. **Angel M, Kimble JB, Pena L, Wan H, Perez DR.** 2013. In vivo selection

22. **Schrauwen EJ, Herfst S, Chutinimitkul S, Bestebroer TM, Rimmelzwaan GF, Osterhaus AD, Kuiken T, Fouchier RA.** 2011. Possible increased pathogenicity of pandemic (H1N1) 2009 influenza virus upon reassortment. Emerg. Infect. Dis. **17:**200–208. http://dx.doi.org/10.3201/eid1702.101268.

23. **van der Vries E, Veldhuis Kroeze EJ, Stittelaar KJ, Linster M, Van der Linden A, Schrauwen EJ, Leijten LM, van Amerongen G, Schutten M, Kuiken T, Osterhaus AD, Fouchier RA, Boucher CA, Herfst S.** 2011. Multidrug resistant 2009 A/H1N1 influenza clinical isolate with a neuraminidase I223R mutation retains its virulence and transmissibility in ferrets. PLoS Pathog. **7:**e1002276. http://dx.doi.org/10.1371/journal.ppat.1002276.

24. **Djikeng A, Halpin R, Kuzmickas R, Depasse J, Feldblyum J, Sengamalay N, Afonso C, Zhang X, Anderson NG, Ghedin E, Spiro DJ.** 2008. Viral genome sequencing by random priming methods. BMC Genomics **9:**5. http://dx.doi.org/10.1186/1471-2164-9-5.

25. **Hoper D, Hoffmann B, Beer M.** 2011. A comprehensive deep sequencing strategy for full-length genomes of influenza A. PLoS One **6:**e19075. http://dx.doi.org/10.1371/journal.pone.0019075.

26. **Qiao C, Liu Q, Bawa B, Shen H, Qi W, Chen Y, Mok CK, Garcia-Sastre A, Richt JA, Ma W.** 2012. Pathogenicity and transmissibility of reassortant H9 influenza viruses with genes from pandemic H1N1 virus. J. Gen. Virol. **93:**2337–2345. http://dx.doi.org/10.1099/vir.0.044040-0.

27. **Manz B, Schwemmle M, Brunotte L.** 2013. Adaptation of avian influenza A virus polymerase in mammals to overcome the host species barrier. J. Virol. **87:**7200–7209. http://dx.doi.org/10.1128/JVI.00980-13.

28. **Mok CK, Yen HL, Yu MY, Yuen KM, Sia SF, Chan MC, Qin G, Tu WW, Peiris JS.** 2011. Amino acid residues 253 and 591 of the PB2 protein of avian influenza virus A H9N2 contribute to mammalian pathogenesis. J. Virol. **85:**9641–9645. http://dx.doi.org/10.1128/JVI.00702-11.

29. **Forbes NE, Ping J, Dankar SK, Jia JJ, Selman M, Keleta L, Zhou Y, Brown EG.** 2012. Multifunctional adaptive NS1 mutations are selected upon human influenza virus evolution in the mouse. PLoS One **7:**e31839. http://dx.doi.org/10.1371/journal.pone.0031839.

30. **Ping J, Keleta L, Forbes NE, Dankar S, Stecho W, Tyler S, Zhou Y, Babiuk L, Weingartl H, Halpin RA, Boyne A, Bera J, Hostetler J, Fedorova NB, Proudfoot K, Katzel DA, Stockwell TB, Ghedin E, Spiro DJ, Brown EG.** 2011. Genomic and protein structural maps of adaptive evolution of human influenza A virus to increased virulence in the mouse. PLoS One **6:**e21740. http://dx.doi.org/10.1371/journal.pone.0021740.

31. **Naffakh N, Tomoiu A, Rameix-Welti MA, van der Werf S.** 2008. Host restriction of avian influenza viruses at the level of the ribonucleoproteins. Annu. Rev. Microbiol. **62:**403–424. http://dx.doi.org/10.1146/annurev.micro.62.081307.162746.

32. **Chakrabarti AK, Pasricha G.** 2013. An insight into the PB1F2 protein and its multifunctional role in enhancing the pathogenicity of the influenza A viruses. Virology **440:**97–104. http://dx.doi.org/10.1016/j.virol.2013.02.025.

33. **Cong YL, Pu J, Liu QF, Wang S, Zhang GZ, Zhang XL, Fan WX, Brown EG, Liu JH.** 2007. Antigenic and genetic characterization of H9N2 swine influenza viruses in China. J. Gen. Virol. **88:**2035–2041. http://dx.doi.org/10.1099/vir.0.82783-0.

34. **Wu LL, Diao YX, Ju XJ, Yu CM, Cui JT.** 2012. Analysis on variation of hemagglutinin genes of sixteen H9N2 subtype avian influenza viruses isolated in Shandong area. Bing Du Xue Bao **28:**272–277. (In Chinese.)

35. **Zhou JP, Ge FF, Liu J, Ju HB, Yang DQ, Wang J, Zhang WY, Liu PH.** 2012. Epidemiological survey and genetic evolution of H9 subtype influenza viruses in Shanghai, China, from 2006 to 2010. Arch. Virol. **157:** 1193–1198. http://dx.doi.org/10.1007/s00705-012-1266-2.

36. **Belser JA, Katz JM, Tumpey TM.** 2011. The ferret as a model organism to study influenza A virus infection. Dis. Model. Mech. **4:**575–579. http://dx.doi.org/10.1242/dmm.007823.

37. **Chou YY, Albrecht RA, Pica N, Lowen AC, Richt JA, Garcia-Sastre A, Palese P, Hai R.** 2011. The M segment of the 2009 new pandemic H1N1 influenza virus is critical for its high transmission efficiency in the guinea pig model. J. Virol. **85:**11235–11241. http://dx.doi.org/10.1128/JVI.05794-11.

38. **Ma W, Bawa LQB, Qiao C, Qi W, Shen H, Chen Y, Ma J, Li X, Webby RJ, García-Sastre A, Richt JA.** 2012. The neuraminidase and matrix genes of the 2009 pandemic influenza H1N1 virus cooperate functionally to facilitate efficient replication and transmissibility in pigs. J. Gen. Virol. **93:**1261–1268. http://dx.doi.org/10.1099/vir.0.040535-0.